cosmetics

MDPI

Article

Molecular-Weight-Driven Penetration of Hyaluronic Acid in Human Skin: A Combined Quantitative and Qualitative Evaluation

Elham Y. Al-Barghouthy [1], Saja Hamed [2], Iman A. Mansi [3], Randa Mansour [4], Nedaa Khlaif [5] and Hatim S. AlKhatib [6,*]

[1] Department of Pharmaceutical Technology and Cosmetics, School of Pharmacy, Middle East University, Amman 11831, Jordan; e.bargouthi@meu.edu.jo
[2] Department of Pharmaceutics and Pharmaceutical Technology, Faculty of Pharmaceutical Sciences, The Hashemite University, Zarqa 13133, Jordan; hamedsh@hu.edu.jo
[3] Department of Clinical Pharmacy and Pharmacy Practice, Faculty of Pharmaceutical Sciences, The Hashemite University, Zarqa 13133, Jordan; iman_mansi@hu.edu.jo
[4] Department of Pharmaceutics & Pharmaceutical Technology, Faculty of Pharmacy, Zarqa University, Zarqa 13110, Jordan; randa_saqer@hotmail.com
[5] Department of Anatomy and Histology, School of Medicine, the University of Jordan, Amman 11942, Jordan; nedaayousef96@gmail.com
[6] Department of Pharmaceutics and Pharmaceutical Technology, School of Pharmacy, the University of Jordan, Amman 11942, Jordan
* Correspondence: h.khatib@ju.edu.jo

Abstract

Hyaluronic acid (HA) is an important extracellular matrix biopolymer whose molecular weight affects skin interactions. This study investigated how low- (LMW), medium- (MMW), and high- (HMW) molecular-weight HA penetrates human skin using fluorescence tagging and ex vivo assays. Fluoresceinamine was conjugated to HA, yielding FA–HA probes with apparent degree-of-substitution values of 7.21% for LMW FA–HA, 4.29% for MMW FA–HA, and 17.20% for HMW FA–HA, with the molecular-weight grades maintained. Because molecular weight and degree of substitution vary together, the results describe these conjugates and do not isolate the effect of molecular weight. In ex vivo experiments with abdominal skin from a single donor (n = 3 discs per grade), no FA–HA reached the receptor compartment of full-thickness skin. Tape stripping showed that total recovery in the skin (1.07–1.59% of the applied dose) and stratum corneum (SC) deposition did not differ significantly between grades. HMW FA–HA was recovered in the viable epidermis in lower amounts than LMW or MMW FA–HA (p = 0.001), and only LMW FA–HA was detected in the dermis (10.21 ± 0.46 µg). Through trypsin-isolated SC, which is likely more permeable than intact SC, LMW and MMW FA–HA were detected in the receptor at 2 h, at 4 h, and at the end of the experiment, whereas HMW FA–HA was barely detectable; cumulative amounts could not be quantified reliably, so release is reported qualitatively. Fluorescence and confocal imaging of sections from one donor showed a similar ranking of fluorescence depth (HMW < MMW < LMW). In the tape-strip profiles, LMW FA–HA was detected beyond strip 10, whereas HMW FA–HA attenuated rapidly after strip 5 (descriptive). These results suggest that, for the tested conjugates, molecular weight is associated with the depth at which HA is found in ex vivo human skin. They are preliminary, come from a single donor, and do not demonstrate a biological or therapeutic effect.

Academic Editor: Elisabetta Esposito

Received: 28 October 2026
Revised: 18 November 2026
Accepted: 23 November 2026
Published: 25 November 2026

Copyright: © 2026 by the authors. Licensee MDPI, Basel, Switzerland. This article is an open access article distributed under the terms and conditions of the Creative Commons Attribution (CC BY) license.

Keywords: hyaluronic acid; tape stripping; fluoresceinamine; penetration; molecular weight; deposition

1. Introduction

Hyaluronic acid (HA) is a biopolymer discovered by Meyer and Palmer in 1934 in bovine vitreous humour [1]. HA is a glycosaminoglycan (GAG) composed of repeating disaccharide units of β-1,4-D-glucuronic acid and β-1,3-N-acetyl-D-glucosamine. It is the simplest and only non-sulfated GAG found in nature, characterised by a high molecular weight and a linear, unbranched structure.

Unlike other GAGs, HA is synthesised at the plasma membrane by hyaluronan synthases (HAS), rather than within the Golgi apparatus [2,3]. HA is abundantly present in the extracellular matrix (ECM) of human and vertebrate tissues, where it plays critical roles in hydration, viscoelasticity, and cellular signalling. While HA does not form covalent bonds with core proteins like traditional proteoglycans, it can associate non-covalently through ionic interactions, often forming large aggregates via link proteins and extended polysaccharide chains.

HA is ubiquitous in cosmetic and medicinal products due to its ability to hydrate skin by attracting and retaining water, creating a moisture barrier. It also supports cell migration, enhances healing, and reduces irritation [4].

A trial with 65 females found that 0.1% sodium hyaluronate formulations of varying molecular weights (50, 130, 300, 800, and 2000 kDa) improved skin hydration and elasticity significantly compared to a placebo after 60 days. The placebo was an oil-in-water emulsion. Pavicic et al. (2011) noted that low-molecular-weight HA formulations effectively reduced wrinkle depth, likely due to better skin penetration [5]. However, according to Cho Lee (2023), more research is needed to prove HA's precise size-dependent skin moisturising effects [6].

Essendoubi et al. (2016) [7] studied the skin permeability of HA of various molecular weights using Raman spectroscopy. They found that 20–50 kDa HA penetrated to 100 μm, reaching the stratum spinosum, while 100–300 kDa HA reached 50 μm (stratum granulosum), and 1000–1400 kDa HA stayed at 25 μm (stratum corneum). The authors concluded that the permeability of HA above 50 kDa is uncertain and requires further study [7].

A qualitative study investigated the skin permeability of fluorescently labelled HA of various molecular weights (2, 8, and 1000 kDa) by comparing fluorescence staining in the skin. Human skin and three-dimensional skin models were employed. Oligosaccharide HA (2 kDa) could pass through the stratum corneum and reach the dermis; however, 1000 kDa HA showed no appreciable fluorescence. To confirm the skin permeability of 2 kDa HA, they measured collagen synthesis and MMP-1 expression and found that both increased [8].

This study aimed to quantitatively investigate how the molecular-weight grade of HA influences its ability to penetrate the human stratum corneum and deposit across full-thickness skin. This was achieved by integrating fluorescence tagging with tape-stripping-based depth-resolved quantification. This combined analytical strategy enabled simultaneous visualisation and quantitative recovery of HA within distinct skin layers, providing a better understanding of how polymer size governs topical diffusion, epidermal retention, and dermal accessibility.

Previous studies assessed HA penetration with label-free Raman spectroscopy [7], qualitative fluorescence staining [8], and tape stripping combined with ELISA [9]. The present work combines a fluorescent HA probe with tape-stripping quantification of

individual skin compartments and imaging of skin sections from the same treatment, as a complementary approach. Its limitations are that the label may alter HA behaviour and that fluorescence cannot distinguish intact from degraded HA.

2. Materials and Methods

2.1. Materials

The following materials were purchased from their respective sources for use in this study: Acetaldehyde (CAS 75-07-0; Sinopec, Beijing, China), Acetic acid glacial (CAS 64-19-7; Surechem Products Ltd., Manchester, UK), Acetone, analytical reagent (CAS 67-64-1; Chem-Lab NV, Zedelgem, Belgium), High-quality agarose (CAS 9012-36-6; TransGen Biotech Co., Ltd., Beijing, China), bromophenol blue (CAS 115-39-9; Virat Lab Fine Chem, Gujarat, India), Stains-All solution (CAS 7423-31-6; Sigma-Aldrich, St. Louis, MO, USA), cyclohexyl isocyanide (CAS 931-53-3; Santa Cruz Biotechnology, Dallas, TX, USA), absolute ethanol (CAS 64-17-5; Scharlab S.L., Sentmenat, Spain), fluoresceinamine (CAS 3326-34-9; Chemscene LLC, Monmouth Junction, NJ, USA), Formamide (CAS 75-12-7; Tokyo Chemical Industry Co., Ltd. (TCI), Tokyo, Japan), and Glycerol (CAS 56-81-5; Gainland Chemical Company, London, UK). Molecular-weight standards were supplied as Select-HA™ LoLadder and HiLadder (Echelon Biosciences Inc., Salt Lake City, UT, USA). The hyaluronic acid used included HyaPoly® Sodium Hyaluronate ≤100–500 kDa, average 300 kDa, and HyaPoly® Sodium Hyaluronate 3–8 kDa, average 5 kDa (Kangcare Bioindustry Co., Ltd., Wuhan, China), while Sodium Hyaluronate ≥1000–2600 kDa, average 1530 kDa (sodium hyaluronate, CAS 9067-32-7) was obtained from Xi'an Otiland Biotechnology Co., Ltd., Xi'an, China. Additional chemicals comprised Hydrochloric acid (CAS 7647-01-0) (Central Drug House (P) LTD., New Delhi, India), and Pre-coated polyacrylamide gel (MBEP, China), along with Sodium acetate (trihydrate) (CAS 6131-90-4; Loba Chemie Pvt. Ltd., Mumbai, India) and Sodium chloride (CAS 7647-14-5; Biochem Chemopharma, Cosne-Cours-sur-Loire, France). Dimethyl sulfoxide (CAS 67-68-5), trypsin (CAS 9002-07-7), phosphate-buffered saline, TAE buffer, DAPI, adhesive tape (Ever Green BOPP) and a regenerated cellulose membrane were also used.

2.2. Preparation of Hyaluronan-Fluorescein Probe (FA-HA)

Hyaluronan was conjugated to fluoresceinamine according to de Belder & Wik (1975) with modifications [10]. A solution of hyaluronate (1 g LMW, MMW; 300 mg HMW) in water (40 mL) was mixed with dimethyl sulfoxide (20 mL). Acetaldehyde (25 µL), cyclohexyl isocyanide (25 µL), and fluoresceinamine (25 mg) were added, keeping the pH between 5.5 and 6.5. After 24 hours at 22 °C, the mixture was poured into 200 mL of ethanol and centrifuged. The precipitated hyaluronate was reprecipitated from water in ethanol with sodium chloride. The dried FA-HA yield was calculated based on the initial HA weight. Thin-layer chromatography (TLC) confirmed the absence of unconjugated dye. Pure dye was spotted along with FA-HA solutions, using chloroform as the mobile phase, and visualised under UV light after 30 minutes.

2.3. Molecular Weight Determination by Gel Electrophoresis and Viscometry

The molecular weight of FA-HA was determined to ensure that no hydrolysis occurred during the tagging reactions. The gel electrophoresis of HA was performed according to the protocol described by Chen, 2018 [11] with some modifications. Briefly, HA samples (1 mg/mL in 10 M aqueous formamide) were mixed with loading buffer (0.005% bromophenol blue and 50% glycerol in 1× TAE), and 15 µL of each sample was loaded per well. In parallel, 25 µL of commercial HA molecular-weight ladders (Select-HA™ LoLadder and HiLadder) (Echelon Biosciences Inc., Salt Lake City, UT, USA) was loaded onto

the gel as markers. A 1% agarose gel (12 × 12 × 0.5 cm) was prepared in 1× TAE, pre-run (80 V, 6 hours) and allowed to equilibrate in 1× TAE buffer overnight. Samples and ladders were electrophoresed at 100 V for 110 minutes. Next, the gel was stained in 0.005% Stains-All working solution for 48 hours in the dark, destained in distilled water for 30 min, and visualised using a Gel Documentation System (Bio-Print TX4, Vilber, Germany) with the MegaCapT software (Vilber Lourmat, Collégien, France) ; molecular weight was analysed using GelAnalyzer 23.1.1 by calculating band retardation factors (Rf) and applying calibration curves generated from ladder standards. FA–HA samples were processed identically but without bromophenol blue or Stains-All staining. FA–HA MMW and LMW were also run on a 20% polyacrylamide gel (PAGE; 40 min, 400 V) to examine the overlap between the LMW and MMW fractions. Viscosity-average molecular weights of native and labelled HA were estimated from the low-shear viscosity of solutions, converting specific viscosity to c[η] with the tabulated relation of Cowman et al. [12] (k′ = 0.4).

2.4. Determining the Degree of Fluoresceinamine Substitution

A calibration curve for the free FA dye was created by preparing 5 dilutions from a fluoresceinamine stock solution (0.1 mg/mL in water). To determine the degree of fluoresceinamine substitution (DS) of FA onto the different HA molecular-weight grades, three independent dilutions were prepared for each of the three FA–HA grades.

Fluorescence intensities of the standards and FA–HA dilutions were measured using a JASCO FP-8550 spectrofluorometer at excitation/emission wavelengths of 492/520 nm, and fluorescence readings were used to calculate the concentration of FA incorporated into the polymer.

The FA:HA molar ratio was determined by first estimating the moles of FA from its fluorescence readings, then calculating the moles of HA by subtracting the FA mass from the total FA–HA mass and dividing by the average molecular weight of the corresponding HA grade.

The degree of substitution (DS) was expressed as the FA:HA molar ratio normalised to the number of disaccharide units per HA chain (Equation (1)) [13,14]. The number of disaccharide units was estimated by dividing the average HA molecular weight by 401 Da, representing the approximate mass of the repeating disaccharide unit composed of D-glucuronic acid and N-acetyl-D-glucosamine. For each MW group, the mean and standard deviation from three independent measurements were calculated and reported. Because the DS was calculated against a free-dye calibration curve and conjugated fluoresceinamine may differ in quantum yield from the free dye, the DS values are apparent values.

$$DS = \frac{\#\ moles\ FA \times MWt\ Disaccharide\ (401)}{Weight\ of\ HA} \times 100\% \quad (1)$$

2.5. Quantitative Analysis of FA-HA

Quantitative determination of FA-HA was achieved by fluorescence spectroscopy through the construction of linear calibration curves using 6–7 standard solutions of FA-HA in water (FA-HA HMW: 0.05–16 μg/mL, FA-HA MMW: 0.2–24 μg/mL and FA-HA LMW: 0.12–19.2 μg/mL) measured in a JASCO FP-8550 spectrofluorometer at excitation/emission wavelengths of 492/520 nm. Because the degree of substitution differed between grades, each grade was quantified against its own FA-HA calibration curve prepared from the same labelled batch.

Method validation adhered to ICH Q2(R1) guidelines, assessing accuracy (recovery) and precision (RSD) at three concentrations. Emission scans confirmed wavelength stability, and LOD and LOQ were calculated from the standard deviation of the response (σ) and the calibration curve's slope (S). Linearity was established through regression

analysis, confirming the procedure's suitability [15]. Calibration standards were prepared in water, and blanks (untreated tape, and epidermis and dermis extracted with water) were subtracted.

2.6. Ex Vivo Permeation and Deposition of FA-HA in Full-Thickness Skin and Stratum Corneum

2.6.1. Membrane Preparation

Samples of adult human skin were obtained from discarded abdominal skin tissue collected following elective abdominoplasty procedures. The study protocol was reviewed and approved by the Institutional Review Board of The Hashemite University, Jordan (Approval No. 28/2/2024/2025, approved on 14 January 2025). All tissue samples were anonymised before use, and no identifiable personal information was collected from donors.

Skin samples were sourced from abdominal donor sites because of their consistent dermal architecture, minimal UV exposure, and surgical accessibility. The collected skin was punched into 3 cm discs and carefully defatted, ensuring the removal of subcutaneous fat while preserving the integrity of the dermal and epidermal layers. Donor details: [Female, Abdominal skin; stored for 2 weeks at −20 °C].

Skin sample thickness was measured using a mechanical caliper on a fixed stand to comply with OECD Guidance Notes on Dermal Absorption (OECD Series on Testing and Assessment No. 156), which requires full-thickness abdominal skin samples to have a final thickness of < 1.00 mm. Samples with a thickness of > 1.00 mm can be used to determine the amount of test chemical in the skin layers rather than its penetration [16]. In the present study, the mean thickness of five of nine discs exceeded 1.00 mm (range of disc means 0.903–1.150 mm; Table 1). As the primary endpoint was deposition in skin layers rather than penetration, these discs were retained, but thickness may have influenced the receptor-compartment results.

Table 1. Representative skin thickness measurements and transepidermal water loss (TEWL) values for HMW, MMW, and LMW HA formulations across three replicates. Skin thickness is expressed in mm (mean ± SD), and TEWL values are reported in g/m²/h.

	1	**2**	**3**
Thickness (mm)	1.00 ± 0.229	0.957 ± 0.051	1.117 ± 0.333
TEWL	6.729 ± 0.091	6.138 ± 0.081	8.145 ± 0.0751
Thickness (mm)	1.017 ± 0.247	0.960 ± 0.085	1.050 ± 0.180
TEWL	6.287 ± 0.07662	5.977 ± 0.08022	5.097 ± 0.0345
Thickness (mm)	1.150 ± 0.229	1.130 ± 0.148	0.903 ± 0.045
TEWL	6.909 ± 0.159	7.3831 ± 0.184	9.165 ± 0.108

The prepared discs were then wrapped in aluminium foil, placed in plastic freezer bags with a zipper, and stored at −20 °C to be used within 2 weeks.

To separate the stratum corneum (SC), frozen full-thickness skin discs were thawed, placed with SC side up in a Petri dish, submerged in a 1% (*w*/*v*) trypsin solution in PBS, sealed, and incubated at 37 °C for up to 48 hours until the SC separated. The isolated SC sheets were then soaked for 2 hours in deionised water to remove traces of trypsin and used immediately in the permeation study (Mansour et al., 2021) [17].

2.6.2. Assessment of Membrane Integrity

Prior to conducting in vitro testing, the integrity of each full-thickness skin and SC disc used was established.

Transepidermal water loss (TEWL) was used to verify the barrier integrity of full-thickness skin discs. The skin samples were placed on aluminium foil, and the TEWL probe (Tewameter TM 300, Courage & Khazaka, Cologne, Germany) was gently placed in contact with the skin surface for 20 seconds; readings were recorded in triplicate under controlled environmental conditions of 25 ± 0.5 °C and 40–50% relative humidity [18]. A threshold of ≤15 g/m²/h, as recommended by FDA guidance, was used to confirm that the skin maintained functional barrier properties [18].

On the other hand, the SC sheets were checked for integrity by microscopic imaging [17]. Because this check detects only gross damage, isolated-SC permeation is reported qualitatively (detected or not detected) and not as absolute permeability.

2.6.3. Deposition and Permeation of FA-HA: Full-Thickness Skin and Stratum Corneum

The deposition of FA-HA in full-thickness skin and its permeation through SC were investigated by mounting the corresponding membrane (thawed full-thickness skin or freshly prepared SC sheets) between the donor and receptor compartments of Franz cells (Orchid Scientific, India) fitted with six diffusion cells (15 mm diameter, 12 mL receptor volume), with a perforated regenerated cellulose membrane used to support the SC sheets.

The receptor compartments were filled with phosphate-buffered saline (PBS) at 32 ± 0.5 °C [9] and stirred at 600 rpm. A 1 mL dose of FA-HA 1% (*w*/*v*) of each of the three molecular-weight grades was applied to the skin surface under non-occluded conditions. Samples (0.2 mL) were taken at 2, 4, and 8 hours in the case of the SC experiments and after 8 hours in the full-thickness skin experiments, replaced with fresh PBS, and analysed using a JASCO FP-8550 spectrofluorometer at 492 nm (excitation) and 520 nm (emission) to calculate the amount of HA-FA that permeated through the membrane. A blank control (membrane without FA-HA) was run in parallel. Receptor samples were diluted into the calibration range before analysis. Because receptor readings of the more permeable grades were above the calibration range and the dilution volumes were not recorded consistently, cumulative amounts could not be quantified reliably, and SC release is reported qualitatively as detected or not detected at each time point.

Furthermore, for the full-thickness skin experiments, the Franz cells were dismantled after 8 h of application, and the skin was removed and cleaned with two dry cotton swabs to prepare it for the tape-stripping experiment as described in Section 2.6.4.

Each test used three skin discs per molecular-weight grade, all obtained from the same donor; these are within-donor (technical) replicates, not independent biological replicates.

2.6.4. Quantitative Deposition: Tape Stripping of Full-Thickness Skin

Tape stripping of full-thickness skin was achieved by applying a 100 g weight onto pieces of Ever Green BOPP adhesive tape placed on the treated area of each skin disc (1.5 cm diameter, ~55.3 g/cm²) for 30 s under controlled conditions (25 ± 0.5 °C, 40–50% RH) [19].

Approximately 20 sequential strips were collected until the SC became translucent, showing the epidermis below. Each strip was removed in a single motion, and all strips, except the first two (discarded to remove residual surface formulation), were extracted in 2 mL of water with agitation for 16 h at 35 ± 0.5 °C.

The residual epidermis was scraped, and the dermis was homogenised and incubated for 24 h at 35 °C before centrifugation (4000 rpm, 60 min). All strip extracts and supernatants of the scraped epidermis and dermis samples were filtered and analysed using a JASCO FP-8550 spectrofluorometer (492/520 nm). Blank controls included untreated tape and epidermis spiked with water. The FA-HA amount per strip was plotted

against tape rank to assess SC depth, and the total SC FA-HA load was calculated as the sum of the amounts in strips 3–20 (equivalent to the area under the amount–rank curve for unit-spaced strips) [20]. Total deposited HA was calculated as the sum of strips 3–20, the scraped epidermis, and the dermis. Amounts were also expressed per unit area of treated skin (1.77 cm^2), and results below the limit of detection are reported as not detected.

Each test used three skin discs per molecular-weight grade, all obtained from the same donor; these are within-donor (technical) replicates, not independent biological replicates.

2.6.5. Qualitative Deposition: Fluorescence Microscopy

To obtain a visual representation of the skin penetration of FA-HA, full-thickness skin samples were treated with FA-HA solutions as described in Section 2.6.3, and the skin was cryosectioned into 5 μm slices and examined with a fluorescence microscope (Nikon Eclipse TE2000-4; Tokyo, Japan). Image acquisition was achieved under controlled conditions (25 ± 0.5 °C). Sections were cut on a cryostat at −25 °C and imaged with a 10× objective (Nikon Eclipse TE2000-4 with a Panasonic Lumix DMC-GF6 camera), with several fields per sample; confocal images used a Plan-Apochromat 63×/1.4 oil objective.

Additional 10–15 μm slices were stained with DAPI, and confocal images were captured using a Zeiss LSM 780 confocal microscope. Excitation lasers at 405 nm and 488 nm targeted DAPI and FITC, with emissions detected in the ranges of 410–500 nm for DAPI and 505–598 nm for FITC. Z-stacks were obtained with a 0.93 μm step size. Penetration depth was defined as the distance from the skin surface to the deepest point at which fluorescence exceeded the mean + 3 SD of untreated skin imaged with identical settings, measured in ImageJ along three lines per section on three sections per grade.

2.7. Statistical Analysis

Data are presented as mean ± SD (n = 3 discs from one donor). Deposition amounts in each layer were compared among the three grades by one-way ANOVA followed by Bonferroni post hoc tests, with $p < 0.05$ considered significant (IBM SPSS Statistics for Windows, Version 26.0 (IBM Corp., Armonk, NY, USA)). Because all discs came from one donor, p-values reflect within-donor reproducibility only. The dermal comparison is descriptive because MMW and HMW values were below the limit of detection.

3. Results

3.1. Fluorescence Tagging

3.1.1. Preparation of HA-FA

Figure A1 shows a schematic representation of the proposed mechanism for FA-HA conjugation [10].

Conjugation proceeds through a four-component Ugi-type reaction between the HA carboxyl group, fluoresceinamine, acetaldehyde and cyclohexyl isocyanide, giving an amide-linked fluorescein side chain; the individual steps are shown in Figure A1 [21]. The pH of the reaction was maintained at 5.5–6.5 to ensure both amine reactivity and HA stability.

The reaction produced yields of 71.7% for HMW, 95% for MMW, and 46.7% for LMW. The low yield of the conjugation of fluoresceinamine to LMW HA was due to the extensive reprecipitation (a total of five precipitation steps in comparison to three steps for HMW and MMW) needed to remove free dye [22]. Upon thin-layer chromatography (TLC) testing of FA-HA samples, the FA-HA species did not migrate, and no free fluoresceinamine spots were observed, confirming successful purification.

3.1.2. Gel Electrophoresis

Figure 1 shows the gel electrophoresis images analysed using GelAnalyzer 23.1.1, where A shows the image of agarose gels displaying the migration profiles of the three molecular-weight grades of HA, the Hiladder®, and the Loladder®. In comparison, B shows the agarose gel images for the three molecular-weight grades of FA-HA. Composite images merging agarose gel lanes of HA and FA-HA are shown in C. The images show identical streams for the HA and FA-HA, suggesting that no substantial depolymerisation of HA occurred during conjugation (gel electrophoresis is semi-quantitative). A similar conclusion can be drawn by comparing the MW of FA-HA to that of HA, as shown in Table 2. The calculated ranges are band-edge estimates that include smear width and overlap with the manufacturer's ranges; they do not prove that molecular weight is identical. Uncropped gels, ladder calibration curves and replicate numbers are provided in the Appendix A.

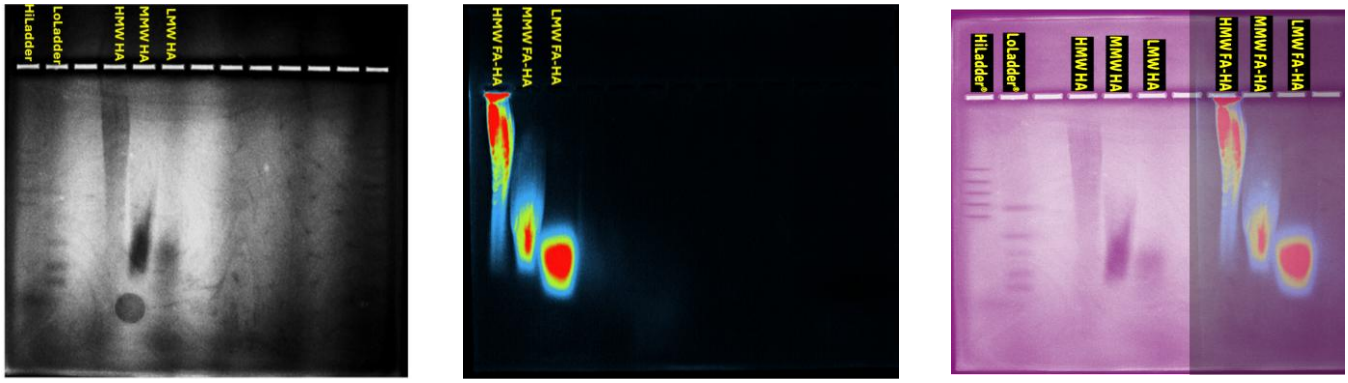

(**a**) (**b**) (**c**)

Figure 1. GelAnalyzer image of agarose gels displaying the migration profiles of (**a**) HMW, MMW, and LMW HA and HiLadder and LoLadder; (**b**) HMW, MMW, and LMW FA-HA; and (**c**) composite image merging agarose gel lanes of native HA and FA-HA, highlighting similarities in migration behaviour.

Table 2. Calculated and reported MW for HA before and after tagging with FA.

	Cal. MW for Untagged HA (kDa)	Cal. MW for Tagged FA-HA (kDa)	Reported MW
HMW	977–3400	489–4810	1000–2600
MMW	93–326	22.3–582	100–500
LMW	5.3–18	4.22–52.3	3–8

These data indicate that FA conjugation did not change the molecular-weight grade of the tagged HA by an amount that agarose gel electrophoresis could resolve.

It is also worth noting that the only major discrepancy between the manufacturer's MW specification and the calculated MW of HA and FA-HA samples exists for the LMW HA. This discrepancy can be attributed to the low resolution of the agarose gel in separating LMW HA [12]. Size-exclusion chromatography with light scattering (SEC-MALS) or GPC would be needed to confirm the molecular-weight distributions.

The gels were calibrated with the HiLadder ($R^2 = 0.9970$) and LoLadder ($R^2 = 0.9996$); the combined-ladder curve used for LMW HA had $R^2 = 0.9903$. The lowest ladder standard is 30.6 kDa, so the LMW values (4–52 kDa) lie below the calibrated range and are extrapolated, and the LMW lane also showed a faint higher-molecular-weight band (about 138 kDa). PAGE showed that the lower boundary of the MMW fraction meets the upper boundary of the LMW fraction. Viscometry gave viscosity-average molecular weights for

native HA and FA–HA of 1324 and 1220 kDa (HMW), 237 and 187 kDa (MMW), and 5.56 and 2.4 kDa (LMW), so all three grades remained in their categories, but the values after labelling were lower by about 8%, 21% and 57%. The larger decrease for LMW may reflect measurement uncertainty (the LMW solution viscosity, 0.70 cP, is at the limit of the method), loss of material during the five precipitation steps, or some chain scission; we therefore do not claim exact preservation of molecular weight.

3.1.3. Determining the Degree of Substitution Using Fluorospectrometric Measurements

Figure 2a shows the emission spectrum for free FA dye vs. FA-HA (all three MW grades showed identical spectra, as detailed in Figure 2b–d). A slight red shift is observed in the excitation and emission wavelengths for the FA dye, changing the excitation wavelength from 490.5 nm for the free dye to 496 nm for FA-HA, and the emission wavelength from 516.5 nm to 522 nm.

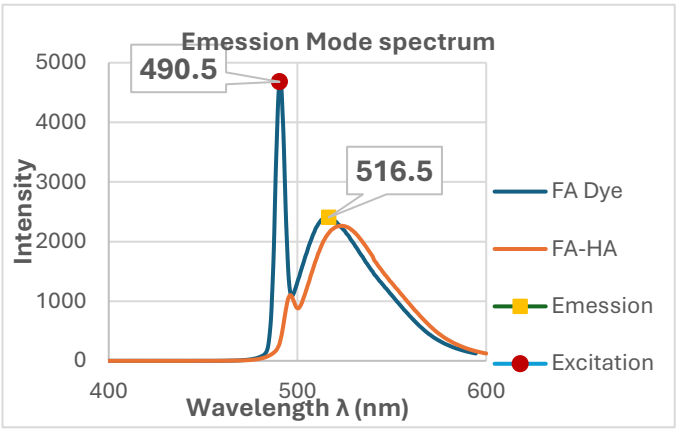

(**a**)

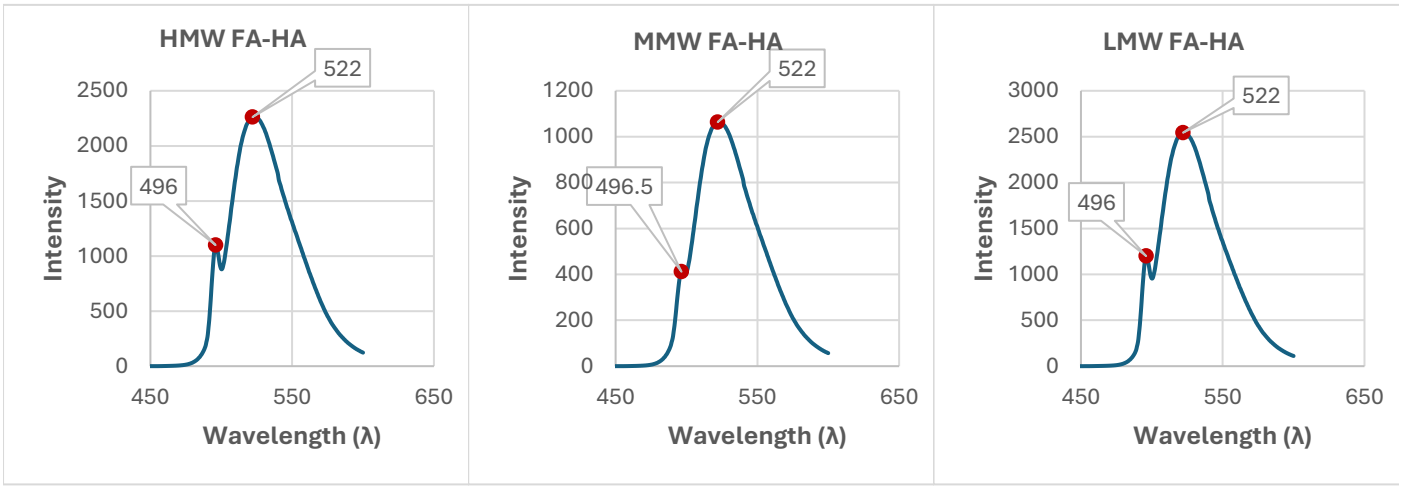

(**b**) (**c**) (**d**)

Figure 2. Emission spectra for free fluoresceinamine dye versus FA-HA. (**a**) shows a slight red shift in the wavelengths for FA-HA excitation and emission. (**b**–**d**) present the emission spectra for FA-HA at high molecular weight (HMW), medium molecular weight (MMW), and low molecular weight (LMW), respectively.

The excitation and emission wavelengths of the free FA dye were utilised to create a calibration curve of intensity versus concentration (y = 106.94x + 3.56, R2 = 0.9987), from which the expected dye concentration was estimated based on the emission intensity from known concentrations of FA-HA (using the wavelengths identified from FA-HA scanning

results). Using the dye concentration in each sample, the degree of substitution (DS%) was calculated, as shown in Table 3.

The calculated DS values (%) were found to be 7.21 ± 0.16 for LMW, 4.29 ± 0.08 for MMW, and 17.20 ± 1.44 for HMW FA-HA, which implies that, out of 100 disaccharides of LMW, MMW, and HMW HA, 7.21, 4.29, and 17.20 are conjugated with FA, respectively.

The DS differed between grades because the reaction used a higher dye-to-HA ratio for HMW (25 mg dye per 300 mg HA) than for LMW and MMW (25 mg per 1 g HA). Because molecular weight and DS therefore vary together, their effects cannot be separated in this study. For LMW HA, the mean of 0.90 dye molecules per chain means that a fraction of the chains is unlabelled and is not detected by fluorescence.

Table 3. Degree of substitution (DS) of FA-HA calculations.

	FA: HA (Mole:Mole)	#Disaccharide/moleHA	(DS), %
FA-HA LMW	0.90	12.469	7.21 ± 0.16
FA-HA MMW	32.06	748.130	4.29 ± 0.08
FA-HA HMW	656.18	3815.461	17.20 ± 1.44

3.1.4. Quantitative Analysis of FA-HA

The calibration curves for FA-HA across high (HMW), medium (MMW), and low (LMW) molecular-weight fractions (Table 4) demonstrated excellent linearity, with R^2 values exceeding 0.997 for all three grades, indicating exceptional consistency across the tested concentration range. Accuracy and precision values were within acceptable analytical limits for all fractions, with FA-HA MMW and HMW showing the highest accuracy (99.44 ± 2.04% and 99.43 ± 3.47%) and FA-HA LMW achieving the best precision (2.72 ± 2.13%). The different DS values do not affect the quantification, because each FA-HA grade was measured against its own calibration curve prepared from the same labelled material (Table 4), so deposited amounts are expressed as FA-HA mass for each grade. This does not remove possible effects of DS on the behaviour of the conjugates in skin (see Section 4).

Table 4. Calibration curves for each HA MW grade.

	FA-HMW	FA-MMW	FA-LMW
Equation	y = 15.751x − 0.4639	y = 4.2898x + 1.097	y = 6.839x + 0.512
Linearity	R^2 = 0.9978	R^2 = 0.9999	R^2 = 0.9999
Accuracy (%)	99.43 ± 3.47	99.44 ± 2.04	98.64 ± 6.18
Precision (%)	2.89 ± 1.78	5.91 ± 3.50	2.72 ± 2.13
LOD (μg/ml)	0.002	0.008	0.005
LOQ (μg/ml)	0.0066	0.024	0.015

Notably, the limits of detection (LOD) and quantification (LOQ) were lowest for FA-HA HMW (0.002 μg/mL and 0.0066 μg/mL, respectively) and highest for FA-HA MMW (0.008 and 0.024 μg/mL), which reflects the different slopes of the calibration curves. Overall, the calibration performance supports the reliability of fluorescence-based quantification for FA-HA across a broad molecular-weight spectrum.

3.2. Ex Vivo Diffusion and Deposition

3.2.1. Membrane Characterisation

The thickness and TEWL measurements of the skin discs used in the deposition studies are presented in Table 1. Across all replicates, the mean disc thickness ranged from 0.903 to 1.150 mm (five of nine discs above 1.00 mm; Table 1), with no significant difference

observed between the different treatment groups. TEWL values of the same skin discs ranged from 5.097 to 9.165 g/m²/h and fell within the expected physiological range for ex vivo human skin under controlled conditions. According to published guidelines, normal TEWL values for healthy skin typically range between 5 and 15 g/m²/h [23,24].

TEWL values were within the acceptance threshold (≤15 g/m²/h) for all discs. Thickness varied between discs, and five of nine exceeded the 1.00 mm criterion.

On the other hand, light microscopy images of the SC sheets showed continuous, unbroken samples without tears or fissures, indicating suitability for permeation studies. This check detects only gross damage and does not confirm functional barrier integrity.

3.2.2. Quantitative Deposition: Tape Stripping of Full-Thickness Skin

As evident from the data presented in Table 5, the deposition profiles of FA–HA across skin layers reveal distinct molecular-weight-dependent distribution patterns. In the stratum corneum, LMW FA-HA exhibited lower mean deposition (88.39 ± 17.57 μg) in comparison to MMW FA-HA (135.61 ± 40.4 μg) and HMW FA-HA (103.92 ± 30.73 μg), but SC deposition did not differ significantly between the grades (Bonferroni $p = 0.331$ to 1.000; Table 6). Strips 1–2 were discarded, so these values exclude the outermost surface layer.

Conversely, LMW FA–HA was recovered from the viable epidermis and dermis, with mean values of 23.36 ± 2.70 μg and 10.21 ± 0.46 μg, respectively, compared to 23.27 ± 4.70 and 3.40 ± 0.5 μg in the deeper epidermis for MMW and HMW FA-HA, while no HMW or MMW FA-HA was detected in the dermis (below the limit of detection). Epidermal amounts were significantly lower for HMW than for LMW or MMW FA-HA ($p = 0.001$), and the dermal difference refers to LMW only.

Total deposited HA (tape strips 3–20, scraped epidermis, and dermis) was numerically highest for MMW (158.88 ± 43.05 μg), followed by LMW (121.95 ± 17.96 μg) and then HMW (107.36 ± 30.24 μg). Total deposition did not differ significantly between the grades (Bonferroni $p = 0.290$ to 1.000; Table 6). Expressed per unit area (1.77 cm²), total deposition was 69.0, 89.9 and 60.8 μg/cm² for LMW, MMW and HMW, respectively (SC 50.0, 76.7 and 58.8; epidermis 13.2, 13.2 and 1.9; dermis 5.8, not detected and not detected μg/cm²). In the tape-strip profiles (amount per strip against strip number), LMW FA-HA was detected beyond strip 10, whereas HMW FA-HA attenuated rapidly after strip 5; these profiles are descriptive and were not compared statistically.

Notably, we detected no fluorescence in the receptor compartment for any FA-HA MW grade, i.e., FA-HA in the receptor was below the limit of detection in all full-thickness skin experiments, consistent with expectations for topical macromolecules.

Table 5. Quantitative deposition of fluorescently labelled hyaluronic acid (FA–HA) across skin layers following topical application of LMW, MMW, and HMW molecular-weight fractions. Values represent mean ± SD ($n = 3$). Values are from three discs of one donor; n.d., not detected.

	FA-LMW	FA-MMW	FA-HMW
Receptor compartment (μg)	n.d.	n.d.	n.d.
Stratum corneum (μg) (strips 3–20)	88.39 ± 17.57	135.61 ± 40.4	103.92 ± 30.73
Epidermis (μg) (scraped epidermis)	23.36 ± 2.70	23.27 ± 4.70	3.40 ± 0.5
Dermis (μg)	10.21 ± 0.46	n.d.	n.d.
Total deposited (μg)	121.95 ± 17.96	158.88 ± 43.05	107.36 ± 30.24
Total deposited (%)	1.22 ± 0.18	1.59 ± 0.43	1.07 ± 0.30

Table 6. Bonferroni-corrected *p*-values for pairwise comparisons (LMW, MMW, HMW) of deposition in each skin layer.

Dependent Variable	LMW–MMW	LMW–HMW	MMW–HMW
SC	0.331	1.000	0.778
Scraped epidermis	1.000	0.001 *	0.001 *
Dermis	<0.001 *	<0.001 *	1.000
Total	0.622	1.000	0.290
SC release	not compared	not compared	not compared

* Statistically significant difference ($p < 0.05$). "Not compared" indicates that no pairwise statistical comparison was performed for SC release.

3.2.3. Permeation Through Stratum Corneum

The results of the FA-HA permeation study through the stratum corneum revealed distinct differences in FA-HA behaviour depending on the molecular weight. After 2 and 4 hours of application, both MMW and LMW FA-HA appeared in measurable amounts in the receptor compartment, while HMW FA-HA was not detected.

At the end of the experiment, LMW and MMW FA-HA were present in the receptor compartment in substantial amounts, whereas HMW FA-HA was barely detectable in two of the three cells; in the third HMW cell, release was higher, which we provisionally attribute to a membrane defect. Cumulative amounts could not be quantified reliably because receptor readings of the more permeable grades were above the calibration range, the dilution volumes were not recorded consistently, and some individual values exceeded the applied dose. Release is therefore reported qualitatively (Table 7), and no difference between LMW and MMW is claimed. These findings are consistent with the published literature, which demonstrates that the molecular weight of HA significantly influences its release and biological activity. High-molecular-weight HA forms denser, more cross-linked networks, resulting in slower diffusion, which makes it suitable for applications requiring prolonged retention, such as a barrier in wound healing. [25,26] In contrast, low-molecular-weight HA crosses isolated SC readily [25,26]. Isolated-SC release is reported qualitatively only (see Section 4).

Table 7. Detection of FA-HA in the receptor compartment below the isolated stratum corneum. Release is reported qualitatively because cumulative amounts could not be quantified reliably (see text).

	HMW	MMW	LMW
Receptor at 2 h	not detected	detected	detected
Receptor at 4 h	not detected	detected	detected
Receptor at end of experiment	trace (<1% of dose) in 2 of 3 cells	detected	detected
Relative release	lowest	high	high

The stability of FA-HA during permeation through SC was ascertained using TLC of samples collected in the receptor compartment and of extracts of the SC after the experiment. It is worth noting that no fluorescent spots corresponding to free fluorescein dye were observed in the FA-HA lanes, indicating that the compound remained intact. This confirms that the fluorescein detected in the Franz cell reservoir originated from the FA-HA conjugate rather than from free or degraded dye.

3.2.4. Qualitative Skin Deposition Assay

In full-thickness skin sections from female abdominal skin, the stratum corneum typically measures 10–20 µm, the viable epidermis extends to about 50–100 µm, and the dermis begins around 100 µm, continuing to several millimetres in depth.

As the degree of substitution varies with different molecular weights, the intensity of fluorescence was not analysed; however, the depth of penetration was considered. Upon fluorescence microscopic evaluation of cross sections of full-thickness skin treated with FA-HA (Figure 3), HMW FA-HA (Figure 3a) shows limited fluorescence penetration of less than 90 µm, indicating confinement to the stratum corneum and upper viable epidermis. This limited diffusion is consistent with the larger molecular size, although the labelling degree also differs between the grades. (Figure 3b), showing the sample treated with MMW FA-HA, shows deeper penetration of around 150 µm, reaching the lower epidermis and dermal–epidermal junction, suggesting intermediate penetration. In Figure 3c, the LMW FA-HA-treated skin shows the deepest penetration, reaching approximately 450 µm and extending into the dermis. These findings align with previous reports indicating that lower-molecular-weight HA exhibits greater diffusivity and tissue penetration due to reduced steric hindrance and enhanced mobility [27]. Depths were measured as described in Section 2.6.5.

Figure 3d illustrates the post-processing of skin section images using ZEN Lite 3.8 (Carl Zeiss Microscopy GmbH, Jena, Germany), where the *Z*-axis was inverted to enhance the spatial visualisation of signal migration, and a single plane was analysed to detect signal migration. This adjustment allows for a clearer interpretation of how FA-HA formulations distribute vertically through the skin layers. By flipping the depth orientation, the fluorescence signals become more distinguishable, especially in regions where overlapping structures may obscure penetration patterns. This processing aids visual interpretation of signal depth and supports the comparative analysis of molecular-weight-dependent diffusion observed in Figure 3a–c (three cross-sectioned slides from one skin sample for each MW).

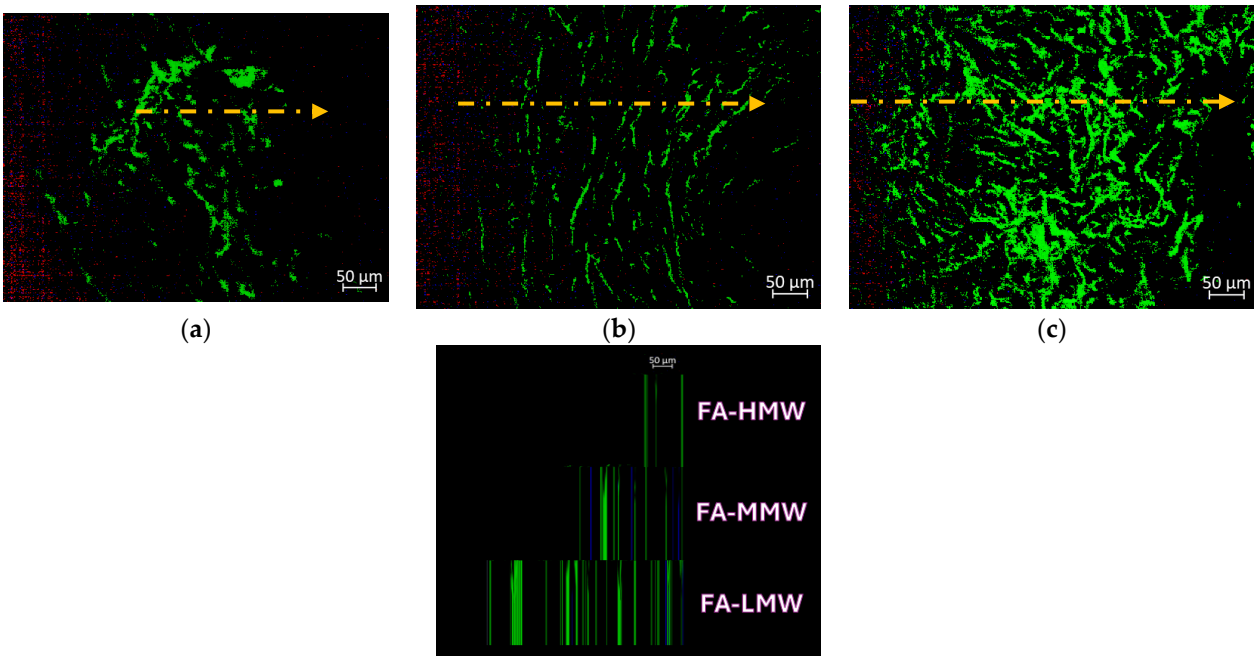

(**a**) (**b**) (**c**)

(**d**)

Figure 3. Fluorescence microscopic images. (**a**–**c**) illustrate the depth of skin penetration achieved by FA-HA formulations of high, medium, and low molecular weight (HMW, MMW, and LMW, respectively) across full-thickness skin sections. Yellow arrows indicate the depth to which FA-HA

travelled through the skin, starting from the surface and extending to the point of deepest penetration. (**d**) displays ZEN Lite-processed images with inverted *Z*-axis orientation to enhance the spatial interpretation of signal migration within the tissue. Three cross-sectioned slides from one skin sample for each MW.

Confocal microscopy images (Figure 4) reveal a clear molecular-weight-dependent pattern of skin penetration by FA-HA formulations, where LMW FA-HA (Figure 4c) demonstrates superior penetration, reaching deeper layers of the dermis, while MMW FA-HA shows intermediate penetration (Figure 4b) and HMW FA-HA remains largely confined to the upper epidermal layers (Figure 4a), suggesting limited penetration. In this single-donor qualitative dataset, these findings align with the known biophysical properties of hyaluronic acid, where lower molecular weights facilitate deeper tissue access.

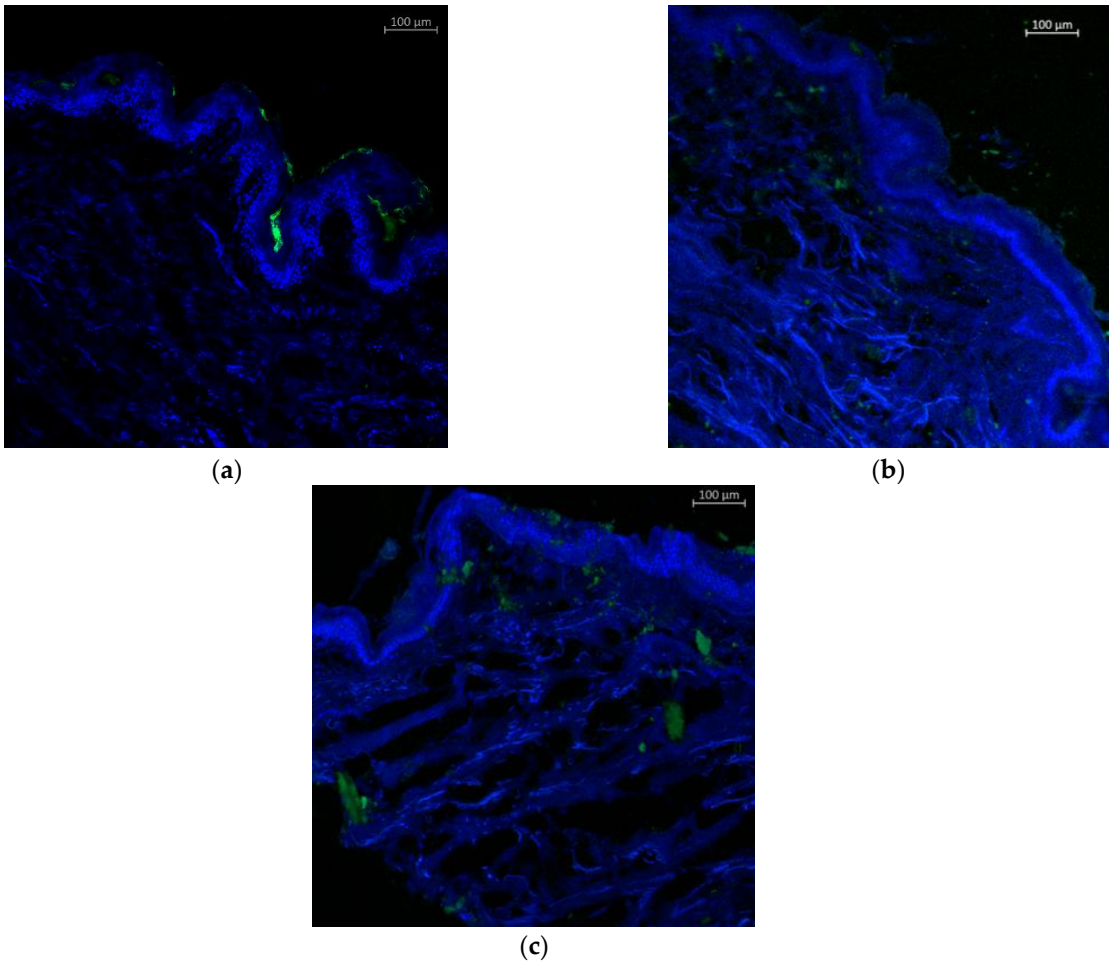

(**a**) (**b**)

(**c**)

Figure 4. Confocal microscopic images of skin penetration by FA-HA formulations. (**a**–**c**) show full-thickness skin sections treated with FA-HA formulations of HMW, MMW, and LMW hyaluronic acid, respectively. Fluorescent signals indicate the depth and distribution of penetration: green fluorescence represents FA-HA localisation and blue fluorescence marks cell nuclei (DAPI staining). The intensity and depth of the green signal vary across panels, with LMW FA-HA (**c**) showing the deepest and most widespread penetration, followed by MMW (**b**) and HMW (**a**), which shows limited surface accumulation. Three cross-sectioned slides from one skin sample for each MW.

4. Discussion

Data from tape stripping of full-thickness skin underscore the importance of molecular weight in modulating HA skin distribution and are aligned with previous studies reporting that lower-molecular-weight HA exhibits greater diffusivity and tissue

penetration due to reduced steric hindrance and enhanced mobility [27] and with Raman spectroscopy studies that showed LMW HA (20–300 kDa) to permeate the stratum corneum, whereas HMW HA remained largely confined to the skin surface [7].

Total deposition was numerically highest for MMW FA-HA but did not differ significantly between the grades, so no ranking can be concluded. If confirmed, retention through interaction with skin components, related to hydrodynamic size or transient entanglement within intercellular lipids, could be one explanation, but this is speculative [28].

Statistical analysis of quantitative data using ANOVA followed by Bonferroni post hoc analysis (Table 6) showed no significant effect of the MW grade of HA on its deposition in the SC despite the lower absolute deposition of the LMW grade. The epidermal levels of deposited HA showed significantly higher penetration of the LMW and MMW HA in comparison to the HMW grade. Total deposition also did not differ between grades. The dermal comparison is descriptive because MMW and HMW values were below the limit of detection.

It is worth noting that up to 48 hours of 1% trypsin at 37 °C might remove or change intercellular proteins and lipids, and that integrity was only assessed by light microscopy, which might make the isolated SC more permeable than the entire SC. Therefore, SC release should be viewed as qualitative evidence, not as absolute permeability. Cumulative amounts in the receptor could not be quantified reliably (readings above the calibration range, inconsistent dilution volumes), so SC release is reported qualitatively and no ranking of LMW and MMW is claimed.

These findings suggest that molecular weight is associated with the depth at which FA-HA is found in ex vivo skin. Whether this applies to unlabelled HA, to other donors, or to formulations used in practice remains to be shown.

The three conjugates differ in degree of substitution (4.3–17.2%) as well as in molecular weight. Higher substitution can change hydrophobicity, chain conformation and interactions with skin components, so a contribution of the label to the differences cannot be excluded. DS does not rise in step with molecular weight (MMW was lowest), which does not by itself exclude an effect. All skin came from one donor, and no HA reached the receptor through full-thickness skin; the findings therefore do not support statements on transdermal delivery.

5. Conclusions

In this single-donor ex vivo study, HMW FA–HA remained mainly in the upper skin layers and was less present in the viable epidermis than LMW or MMW FA–HA. Only LMW FA–HA was detected in the dermis. Total deposition and SC deposition did not differ significantly between grades, and no FA–HA crossed full-thickness skin. Because the conjugates differ in degree of substitution, a contribution of the label to these differences cannot be excluded.

To our knowledge, combining a fluorescent HA probe with tape-stripping quantification and imaging in the same experiment adds quantitative depth information to earlier label-free and qualitative studies. The approach needs confirmation with several donors, matched degrees of labelling and validated membrane integrity before it can inform formulation design.

6. Limitations

All skin came from one donor, so the three discs per grade are within-donor replicates and the *p*-values do not account for donor variability.

The three conjugates differ in both molecular weight and degree of substitution (apparent DS 4.3–17.2%), and DS was estimated against a free-dye calibration. Molecular weight was assessed by semi-quantitative agarose gel electrophoresis, which resolves LMW HA poorly (LMW values are extrapolated below the lowest ladder standard), and viscometric molecular weight fell by about 8%, 21% and 57% (HMW, MMW, LMW) after labelling.

Skin was frozen and thawed. Trypsin-isolated SC, whose integrity was checked only by light microscopy, is probably more permeable than intact SC, so SC permeation is reported qualitatively.

The first two tape strips were discarded, recovery from tape and tissue was not determined, and surface residue was not measured, so the mass balance is incomplete. Microscopy is qualitative, from sections of one donor, and fluorescence intensity was not compared between grades. Fluorescence cannot distinguish intact FA-HA from degraded fragments.

Author Contributions: E.Y.A.-B.: conceptualisation, investigation (all experimental work), formal analysis, and writing of the original draft. S.H.: supervision of manuscript editing and skin penetration tests. I.A.M.: investigation (gel electrophoresis). R.M.: investigation (skin membrane characterisation). N.K.: microscopic examination and the qualitative part of the study. H.S.A.: manuscript review and editing, supervision of the results and discussion. All authors have read and agreed to the published version of the manuscript.

Funding: The Deanship of Academic Research at the University of Jordan provided financial support through grant 39-2023/2024.

Institutional Review Board Statement: Samples of adult human skin were obtained from discarded abdominal skin tissue collected following elective abdominoplasty procedures. The study protocol was reviewed and approved by the Institutional Review Board of The Hashemite University, Jordan (Approval No. 28/2/2024/2025, approved on 14 January 2025). All tissue samples were anonymised before use, and no identifiable personal information was collected from donors.

Informed Consent Statement: Written informed consent was waived by the Institutional Review Board because samples of adult human skin were obtained from discarded abdominal skin tissue collected following elective abdominoplasty procedures. All tissue samples were anonymised before use, and no identifiable personal information was collected from donors. No patient permission was sought.

Data Availability Statement: Data supporting the findings of this study are available upon request from the authors.

Acknowledgments: The authors would like to acknowledge the Deanship of Academic Research at the University of Jordan for the financial support provided through grant 39-2023/2024. During the preparation of this manuscript, the authors used Claude (Anthropic) to assist with formatting the manuscript to comply with the journal submission requirements and to improve language clarity and readability. The AI tool was not used for data analysis, interpretation of results, or generation of scientific conclusions. The authors critically reviewed and edited all outputs and take full responsibility for the content of this publication.

Conflicts of Interest: The authors report no conflicts of interest.

Abbreviations

The following abbreviations are used in this manuscript:

DS	Degree of substitution
FA-HA	Fluoresceinamine-labelled hyaluronic acid

HA	Hyaluronic acid
MW	Molecular weight
LMW, MMW, HMW	Low, medium and high molecular weight
SC	Stratum corneum
TEWL	Transepidermal water loss

Appendix A

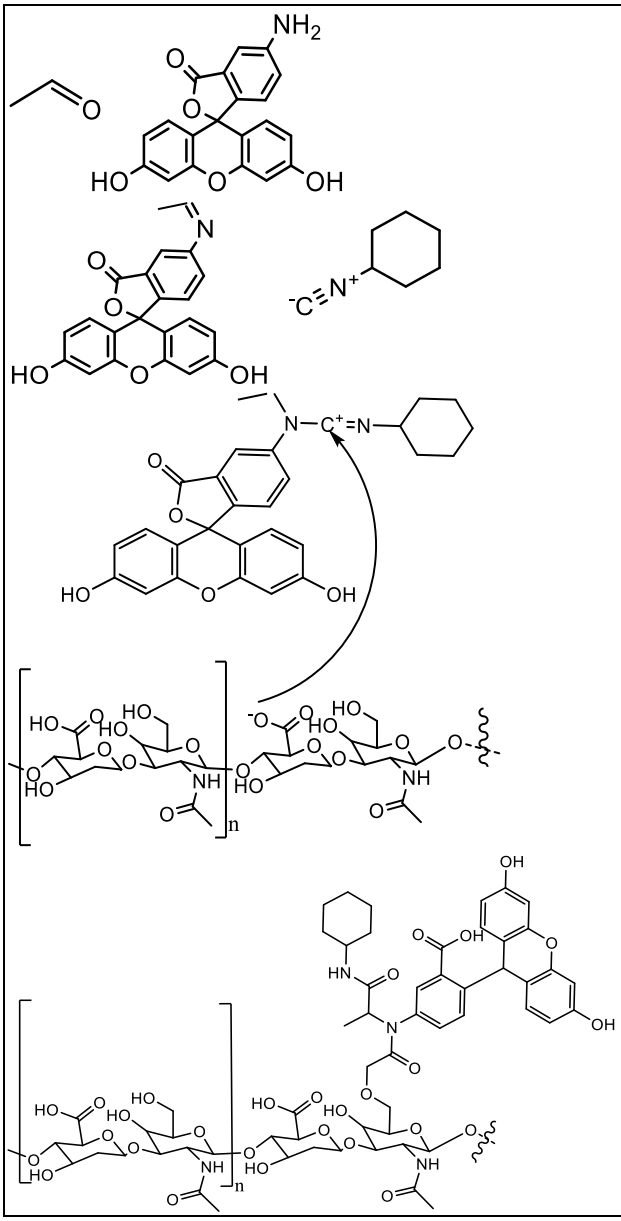

Fluoresceinamine + Acetaldehyde → imine

Cyclohexyl isocyanide attacks imine → nitrilium ion

HA carboxylate attacks nitrilium ion → amide product

Mumm rearrangement, where the acyl group migrates to the amine, yielding the amide linkage between HA and the fluorescein-containing side chain. Reaction pH and the covalent attachment open the fluorescein lactone and prevent reclosure. Lactone opening causes FA to fluoresce.

Figure A1. Schematic representation of the proposed mechanism for FA-HA conjugation.

References

1. Meyer, K.; Palmer, J.W. The polysaccharide of the vitreous humor. *J. Biol. Chem.* **1934**, *107*, 629–634.
2. Kogan, G.; Šoltés, L.; Stern, R.; Gemeiner, P. Hyaluronic acid: A natural biopolymer with a broad range of biomedical and industrial applications. *Biotechnol. Lett.* **2007**, *29*, 17–25. https://doi.org/10.1007/s10529-006-9219-z.
3. Fraser, J.R.E.; Laurent, T.C.; Laurent, U. Hyaluronan: Its nature, distribution, functions and turnover. *J. Intern. Med.* **1997**, *242*, 27–33. https://doi.org/10.1046/j.1365-2796.1997.00170.x.
4. Juncan, A.M.; Moisă, D.G.; Santini, A.; Morgovan, C.; Rus, L.-L.; Vonica-Țincu, A.L.; Loghin, F. Advantages of hyaluronic acid and its combination with other bioactive ingredients in cosmeceuticals. *Molecules* **2021**, *26*, 4429. https://doi.org/10.3390/molecules26154429.

5. Pavicic, T.; Gauglitz, G.G.; Lersch, P.; Schwach-Abdellaoui, K.; Malle, B.; Korting, H.C.; Farwick, M. Efficacy of cream-based novel formulations of hyaluronic acid of different molecular weights in anti-wrinkle treatment. *J. Drugs Dermatol. JDD* **2011**, *10*, 990–1000.
6. Cho Lee, A.-R. Size matters: Differential property of hyaluronan and its fragments in the skin-relation to pharmacokinetics, immune activity and wound healing. *J. Pharm. Investig.* **2023**, *53*, 357–376.
7. Essendoubi, M.; Gobinet, C.; Reynaud, R.; Angiboust, J.F.; Manfait, M.; Piot, O. Human skin penetration of hyaluronic acid of different molecular weights as probed by Raman spectroscopy. *Ski. Res. Technol.* **2016**, *22*, 55–62. https://doi.org/10.1111/srt.12228.
8. Abe, Y.; Seino, S.; Kurihara, H.; Kage, M.; Tokudome, Y. 2-kDa hyaluronan ameliorates human facial wrinkles through increased dermal collagen density related to promotion of collagen remodeling. *J. Cosmet. Dermatol.* **2023**, *22*, 320–327.
9. Grégoire, S.; Man, P.D.; Maudet, A.; Le Tertre, M.; Hicham, N.; Changey, F.; Gaëlle, B.-S.; Tran, C.; Laurence, V. Hyaluronic acid skin penetration evaluated by tape stripping using ELISA kit assay. *J. Pharm. Biomed. Anal.* **2023**, *224*, 115205.
10. de Belder, A.N.; Wik, K.O. Preparation and properties of fluorescein-labelled hyaluronate. *Carbohydr. Res.* **1975**, *44*, 251–257.
11. Chen, J.-W.E.; Pedron, S.; Shyu, P.; Hu, Y.; Sarkaria, J.N.; Harley, B.A.C. Influence of hyaluronic acid transitions in tumor microenvironment on glioblastoma malignancy and invasive behavior. *Front. Mater.* **2018**, *5*, 39.
12. Cowman, M.K.; Chen, C.C.; Pandya, M.; Yuan, H.; Ramkishun, D.; LoBello, J.; Bhilocha, S.; Russell-Puleri, S.; Skendaj, E.; Mijovic, J.; et al. Improved agarose gel electrophoresis method and molecular mass calculation for high molecular mass hyaluronan. *Anal. Biochem.* **2011**, *417*, 50–56.
13. Liu, X.-L.; Zhu, C.-F.; Liu, H.-C.; Zhu, J.-M. Quantitative analysis of degree of substitution/molar substitution of etherified polysaccharide derivatives. *Des. Monomers Polym.* **2022**, *25*, 75–88.
14. Wu, Y.; Zhao, S.; Wang, J.; Chen, Y.; Li, H.; Li, J.-P.; Kan, Y.; Zhang, T. Methods for determining the structure and physicochemical properties of hyaluronic acid and its derivatives: A review. *Int. J. Biol. Macromol.* **2024**, *282*, 137603.
15. Agency, E.M. ICH Topic Q 2 (R1) validation of analytical procedures: Text and methodology. *Prescrire Int.* **1995**, *20*, 278.
16. OECD. *Guidance Notes on Dermal Absorption*; Series on Testing and Assessment no. 156; OECD: Paris, France, 2011; Volume 36, pp. 1–72.
17. Mansour, R.S.; Hamdan, I.I.; Salem, M.S.H.; Khalil, E.A.; Sallam, A.A. HPLC method development/validation and skin diffusion study of caffeine, methyl paraben and butyl paraben as skin–diffusing model drugs. *PLoS ONE* **2021**, *16*, e0247879.
18. Administration, U.F.a.D. In vitro permeation test studies for topical drug products submitted in ANDAs guidance for industry. 2022, October. https://www.fda.gov/media/162475/download, accessed 24 November 2026
19. Hughes, A.; Tawfik, S.S.; Baruah, K.P.; O'tOole, E.A.; O'sHaughnessy, R.F.L. Tape strips in dermatology research. *Br. J. Dermatol.* **2021**, *185*, 26–35.
20. Nallagundla, S.; Patnala, S.; Kanfer, I. Application of an optimized tape stripping method for the bioequivalence assessment of topical acyclovir creams. *AAPS PharmSciTech* **2018**, *19*, 1567–1573.
21. Ugi, I. *Isonitrile Chemistry*; Elsevier: Amsterdam, The Netherlands, 2012; Volume 20.
22. Luo, Y.; Prestwich, G.D. Synthesis and selective cytotoxicity of a hyaluronic acid− antitumor bioconjugate. *Bioconjugate Chem.* **1999**, *10*, 755–763.
23. Fluhr, J.W.; Wiora, G.; Nikolaeva, D.G.; Miséry, L.; Darlenski, R. In vivo transepidermal water loss: Validation of a new multisensor open chamber water evaporation system Tewameter TM Hex. *Ski. Res. Technol.* **2023**, *29*, e13307.
24. Primavera, G.; Fluhr, J.W.; Berardesca, E. Standardisation of measurements and guidelines. In *Bioengineering of the Skin: Water and the Stratum Corneum*; CRC Press: Boca Raton, FL, USA, 2005; pp. 84–95.
25. Waggett, S.; Lyles, E.; Schlesinger, T. Update on Low-Molecular Weight Hyaluronic Acid in Dermatology: A Scoping Review. *Dermatology* **2024**, *12*, 134–146.
26. Mazzucco, A. Hyaluronic acid: Evaluation of efficacy with different molecular weights. *Int. J. Chem. Res* **2019**, *1*, 13–18.
27. Chylińska, N.; Maciejczyk, M. Hyaluronic Acid and Skin: Its Role in Aging and Wound-Healing Processes. *Gels* **2025**, *11*, 281.
28. Cilurzo, F.; Vistoli, G.; Gennari, C.G.M.; Selmin, F.; Gardoni, F.; Franzè, S.; Campisi, M.; Minghetti, P. The role of the conformational profile of polysaccharides on skin penetration: The case of hyaluronan and its sulfates. *Chem. Biodivers.* **2014**, *11*, 551–561.

Disclaimer/Publisher's Note: The statements, opinions and data contained in all publications are solely those of the individual author(s) and contributor(s) and not of MDPI and/or the editor(s). MDPI and/or the editor(s) disclaim responsibility for any injury to people or property resulting from any ideas, methods, instructions or products referred to in the content.